FRACTIONATION AND THERMAL CHARACTERIZATION OF HEMICELLULOSES FROM BAMBOO (*PHYLLOSTACHYS PUBESCENS MAZEL*) CULM

Hong Peng,* Zhengrong Hu, Ziping Yu, Jinsheng Zhang, Yuhuan Liu, Yiqin Wan, and Roger Ruan

Water-soluble hemicelluloses and eight alkali-soluble hemicelluloses were fractionated from bamboo (*Phyllostachys pubescens Mazel*) culm with hot distilled water, 2% NaOH, 2% KOH, 5% NaOH, and 5% KOH aqueous solution. The chemical structures, as analyzed employing FTIR spectrometry, suggested that all the hemicelluloses were likely to be comprised of arabinoxylans associated with lignin more or less. Thermal analysis for hemicelluloses was carried out using TG-DTG method under nitrogen atmosphere at a heating rate of 10 °C/min, and first-order kinetics was evaluated. The major pyrolysis was focused at 187-346 °C, with activation energy ranging from 23.77 to 45.02 kJ/mol. The alkali-soluble fractions, being soluble in solution only at pH higher than 5.5, presented lower thermal stability and higher values of activation energy and pre-exponential factor than the alkali-soluble fractions remaining soluble in alkaline solution at pH lower than 5.5 and insoluble in ethanol. The chemical property of the hemicellulose fractions may greatly influence the thermal characteristics.

Keywords: Bamboo culm; Hemicelluloses; Chemical structure; Kinetics; Pyrolysis

Contact information: EngineeringResearchCenter for Biomass Conversion, Ministry of Education, NanchangUniversity, Nanchang, Jiangxi330047, P R. China
** Corresponding author:* penghpez@yahoo.com.cn

Nomenclature

A pre-exponential factor (min^{1-})
E activation energy (J/mol)
R universal gas constant (8.314 J/mol·K)
T thermodynamic temperature (K)
m_0 initial sample mass (mg)
m_T sample mass at temperature T (mg)
m_∞ residue mass at the end of process (mg)
n reaction order
K reaction rate constant (min^{-1})
a conversion ratio

Greek letters

A mass fraction at temperature T
r heating rate (°C/min)

Subscript

1 first pyrolysis stage
2 second pyrolysis stage
3 third pyrolysis stage
0 initial
∞ final or infinite

INTRODUCTION

Bamboo, which can be classified as a fast-growing lignocellulosic biomass, is widely distributed in the world, especially in Asia, including China (Market Report No.11A001 2001), Thailand (So and Wong 1998), and India (Shanmughavel and Francis 1996). Bamboo plays an essential role in preventing soil erosion and conserving soil moisture. Besides, bamboo has good fiber quality for paper-making, and it shares a number of desirable fuel characteristics with other bio-energy feed stocks. Due to its abundance, renewability, and biodegradation, much attention has been concentrated on bamboo used as potential resource of value-added by-products and bio-energy feedstock in paper-making industry, material industry, energy industry, etc. (Scurlock et al. 2000; Rousset et al. 2011).

Various technologies for utilization of biomass through biological and chemical conversion have been developed (Yu et al. 2008; Huang et al. 2008; Velmurugan and Muthukumar 2011; Gírio et al. 2010). In particular, thermal chemical processes are widely regarded as promising methods for utilization of biomass. Cellulose, hemicellulose, and lignin are the basic constituents in lignocellulosic biomass, and their thermal behavior is highly related to biomass degradation in a high-temperature environment. The behavior of thermal decomposition of cellulose has been extensively investigated in the literature (Shen and Gu 2009; Patwardhan et al. 2011). Hemicellulose is the least stable among the main lignocellulosic biomass components, and it is easy to hydrolyze and pyrolyze (Xu and Hanna 2010; Yang et al. 2007). As the second most abundant polysaccharide in the plant cell wall, hemicellulose is considered to associate with cellulose and lignin via hydrogen bonds and covalent bonds, providing the binding for structural support to the secondary cell wall in the plant (Gírio et al. 2010). Much work has been done to study the thermal properties of hemicellulose (Peng and Wu 2010; Shen et al. 2010). However, hemicellulose is a matrix of different polysaccharides. Hemicelluloses from different biomass might have different physical and chemical properties (Sun et al. 2004; Sun et al. 2011; Wen et al. 2011). Even though from the same plant, the properties, such as molecular weight, content of associated lignin, and neutral sugar composition, are probably affected by different separation methods (Sun et al. 2004; Sun et al. 2011). For example, according to Sun et al. (2011), there is also minor difference of thermal properties owing to the structural inhomogeneity of different fractions from *Tamarix austromongolica.*

Bamboo is mainly composed of three different types of polymers, including cellulose (40-48%), hemicellulose (25-30%), and lignin (11-27%) (Scurlock et al. 2000). Bamboo hemicellulose is a heterogeneous polymer comprised of pentoses (xylose, arabinose), hexoses (mannose, glucose, and galactose), and uronic acids (Wen et al. 2011; Edashige and Ishii 1998). Therefore, in order to provide a useful insight into thermal treatment of bamboo, it is meaningful to investigate the thermal properties of bamboo hemicellulose. Understanding the pyrolysis behavior of bamboo hemicellulose is of practical importance to better explore the underlying processes and to improve the design for utilization of bamboo as feedstock in many areas of application, such as bioenergy.

The aim of the present work was to elucidate the thermal pyrolysis characteristics of water–soluble and alkali–soluble hemicelluloses sequentially isolated from bamboo

(*Phyllostachyspubescens Mazel*) culm in detail using the non-isothermal thermogravimetry method coupled with derivative thermogravimetry (TG-DTG) analysis. The pyrolytic behaviour between the hemicelluloses was compared. The chemical structures of the hemicelluloses were also estimated employing Fourier transform infrared spectrometry (FTIR).

EXPERIMENTAL

Materials

One-year-old bamboo was collected from a farm (Guanxi Village, Meiling Town, Nanchang City, China). The bamboo culm sampled was a mixture of the three sections, including the bottom, the middle, and the top of the bamboo. After being fully dried in sunlight, the culm was cut into small pieces and ground to pass a 40 mesh screen followed by a 100 mesh screen, then dried further in an oven at 50 °C for 12 h prior to use. The final moisture content was 7.90%. The principal composition (%, w/w) of the bamboo culm was analyzed as hemicellulose 29.82%, cellulose 43.54%, Klason lignin 18.18%, and ash 1.44% on a dry weight basis, according to the method for measuring the chemical composition of wheat straw described in the literature (Lawther et al. 1995). All chemicals used were of analytical grade and purchased from Tianjin Chemical Reagent Factory (Tianjin, China).

Methods

Fractionation of hemicelluloses from bamboo culm

The method for hemicellulose fractionation from bamboo culm was adapted from the literature (Sun et al. 2001, 2004, 2011) with partial modification. The scheme is shown in Fig.1. The bamboo powder was first extracted with toluene-ethanol (2:1, v/v) at 95 °C for 6 h in a Soxhlet apparatus. The dewaxed sample was treated with sodium chlorite in acidic mixture (pH 4.2 to 4.7, adjusted with acetic acid) for 3 h at 75 °C. The obtained holocellulose was sequentially extracted with hot distilled water, 2% NaOH, 2% KOH, 5% NaOH, and 5% KOH aqueous solution. Finally, water-soluble hemicelluloses BHW, alkali-soluble hemicellulosic fractions BH1, BH2, BH3, BH4, BH5, BH6, BH7, and BH8 were obtained by means of the separation steps shown in Fig. 1. The alkali-soluble hemicelluloses BH1, BH2, BH3, and BH4 were soluble in solution only at pH value higher than 5.5. The fractions BH5, BH6, BH7, and BH8 remained soluble in alkaline solution upon acidification to pH 5.5 with acetic aicd, and were insoluble in 95% ethanol. The fractions BH1 and BH5 were soluble in 2% NaOH aqueous solution, while the fractions BH2 and BH6 were soluble in 2% KOH aqueous solution. The treatment with 5% KOH resulted in the fractions of BH3 and BH7. The hemicellulosic fractions BH4 and BH8 were separated using 5% NaOH solution. The yields of hemicelluloses were given on a dry weight basis.

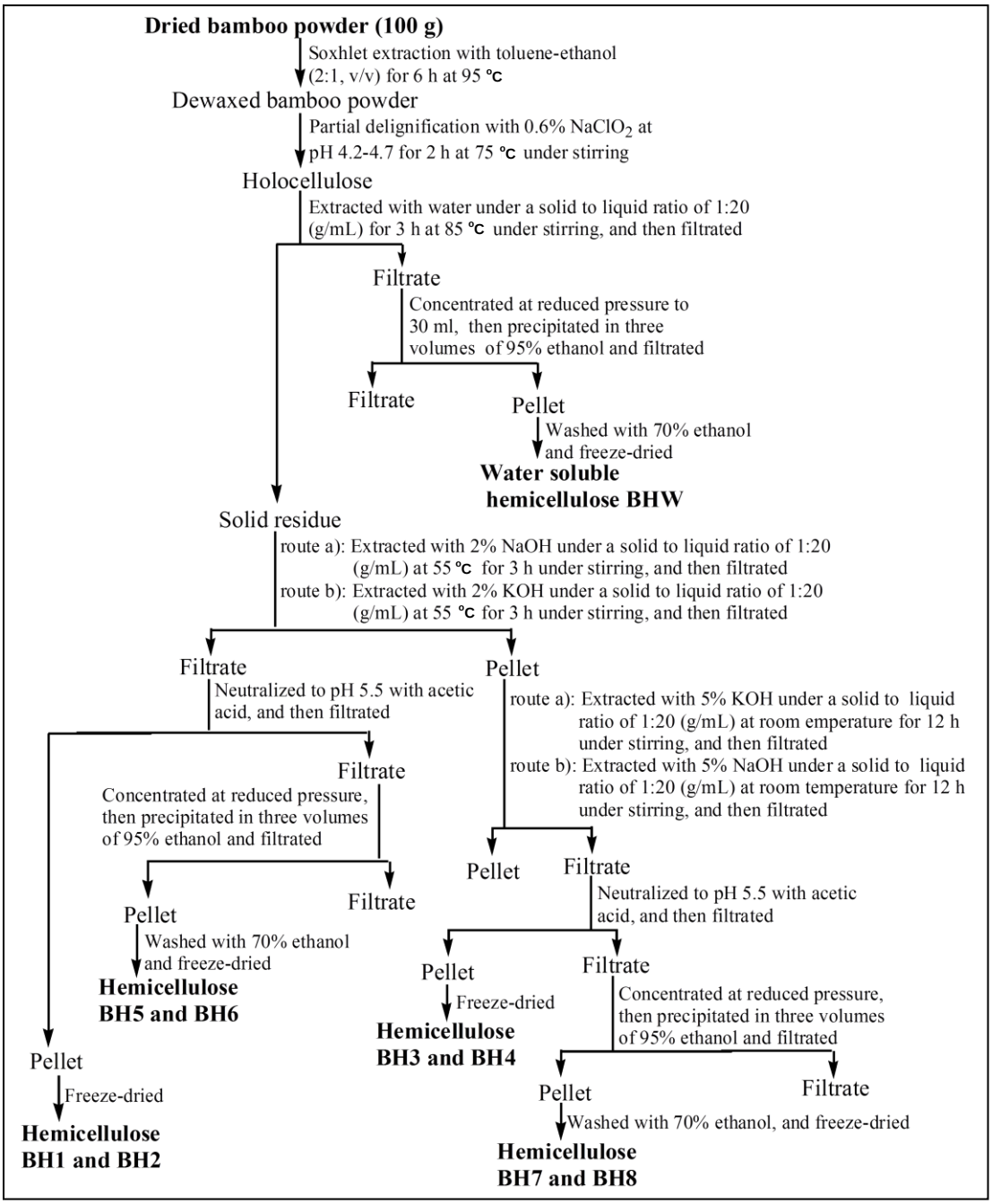

Fig.1. Scheme for hemicellulose fractionation from bamboo culm

FT-IR analysis

For FT-IR measurements, hemicellulose samples were blended with KBr to form pellets, and the spectra were obtained on a Nicolet 7500 FT-IR spectrophotometer (Thermo Nicolet Corporation, USA) in the range of 4000 to 400 cm^{-1} at 4 cm^{-1} resolution.

Thermal analysis

Thermal analysis of the hemicelluloses was evaluated by thermogravimetry carried out on a TG/DTA PYRIS DIAMOND instrument (PE Corporation, USA). The measurements were recorded under nitrogen atmosphere at a flow rate of 50 mL/min at a constant heating rate of 10 °C/min from room temperature up to a final temperature of 700 °C. Considering the variety of initial sample mass at small range having negligible influence on biomass pyrolysis (Yang et al. 2004), approximately 1.2 to 6.5 mg initial weight of hemicelluloses was taken randomly for each sample, as depicted in Table 1. Calcined Al_2O_3 was used as a reference material in all experiments. All thermal process for each sample was performed only once.

Table1. Initial Weight of Hemicellulose Samples Used for Thermal Analysis

Hemicelluloses	BHW	BH1	BH2	BH3	BH4	BH5	BH6	BH7	BH8
Weight (mg)	6.483	3.712	5.283	1.242	3.716	4.291	5.577	1.529	2.343

RESULTS AND DISCUSSION

Yield of Hemicelluloses

The yields of the hemicelluloses based on the original hemicellulose content in bamboo culm are given in Table 2. As indicated by the data in Table 2, treatment of the holocellulose with distilled water at 85 °C for 3 h yielded 4.16% of the original hemicellulose. Alkaline treatment leads to saponification of ester linkages in hemicellulose, along with disruption of hydrogen bonds linking hemicellulose with cellulose, resulting in solubilization and condensation of lignin as well as cellulose swelling. The yields of alkali-soluble hemicelluloses ranged from 2.11% to 15.63%. Under the same extraction conditions, the yields of hemicelluloses extracted with NaOH solution were higher than those of hemicellulosic fractions extracted with KOH solution. It is well known that the basicity of NaOH is stronger than that of KOH considering the same mass concentration in aqueous solution. Hemicelluloses are more easily released from the plant cell walls with stronger alkaline treatment (Sun et al. 2001). Hence, extraction with NaOH led to higher hemicellulose yields under the same extraction conditions.

Table 2. Yields of Hemicelluloses (% dry matter) Solubilized During the Treatments of Bamboo Culm Powder

Hemicelluloses	Extractant	Yield (%)	Total yield (%)
BHW	Hot distilled water	4.16	67.61
BH1	2% NaOH	5.50	
BH2	2% KOH	4.53	
BH3	5% KOH	6.71	
BH4	5% NaOH	8.42	
BH5	2% NaOH (ethanol insoluble)	15.63	
BH6	2% KOH (ethanol insoluble)	14.55	
BH7	5% KOH (ethanol insoluble)	2.11	
BH8	5% NaOH (ethanol insoluble)	6.00	

The total yield of hemicelluloses from bamboo culm under the experimental conditions mentioned above accounted for 67.61% of the total hemicellulose content of original bamboo powder. The total yield of alkali-soluble fractions accounted for the majority of hemicelluloses separated.

Chemical Structure of Hemicelluloses

Figure 2 gives the FT–IR spectra of the hemicellulosic fractions separated from the bamboo culm. The presence of a prominent band at about 3425 cm^{-1} was due to the hydroxyl stretching vibrations of the hemicelluloses and water involved in hydrogen bonding (Revanappa et al. 2010). The weak adsorption attributed to the C–H stretching vibrations was at around 2934 cm^{-1} (Revanappa et al. 2010). The band at 1739 cm^{-1} indicated the presence of acetyl or uronic ester groups of the water–soluble hemicelluloses. The absence of this absorption at 1739 cm^{-1} in all the eight alkali-soluble hemicellulose spectra implied that the acetyl or uronic ester groups had been completely cleaved when alkaline solution was used as extractant (Sun et al. 2002). The adsorption at 1640 cm^{-1} was principally associated with absorbed water. The bands at 1577 and 1510 cm^{-1} originated from aromatic skeletal vibrations in associated lignin, indicating that the hemicelluloses isolated were slightly contaminated with small amounts of lignin (Vazquez et al. 1997). The peaks at 1411, 1377, 1335, 1252, 1048, and 980 cm^{-1} were associated with hemicelluloses. The band at 1411 cm^{-1} indicated the presence of carboxylate groups (Chaa et al. 2008). The bands between 1130 and 1000 cm^{-1} were typical of xylans (Xiao et al. 2001). The sharp band at 897 cm^{-1} was due to the C-1 group frequency, which was characteristic of *β*–glycosidic linkages between the sugar units of hemicelluloses (Kačuráková et al. 2000). It confirmed that the hemicellulose backbone was built up *β*–linked xylose units. The presence of arabinosyl side chains was indicated by low-intensity shoulders at 1162 and 980 cm^{-1} (Kačuráková et al. 1998). The small shoulder peak at 1162 cm^{-1} in all the spectra of hemicelluloses corresponded to the glycosidic bond vibrations of arabinosyl side chain in the anometric region (Xiao et al. 2001).

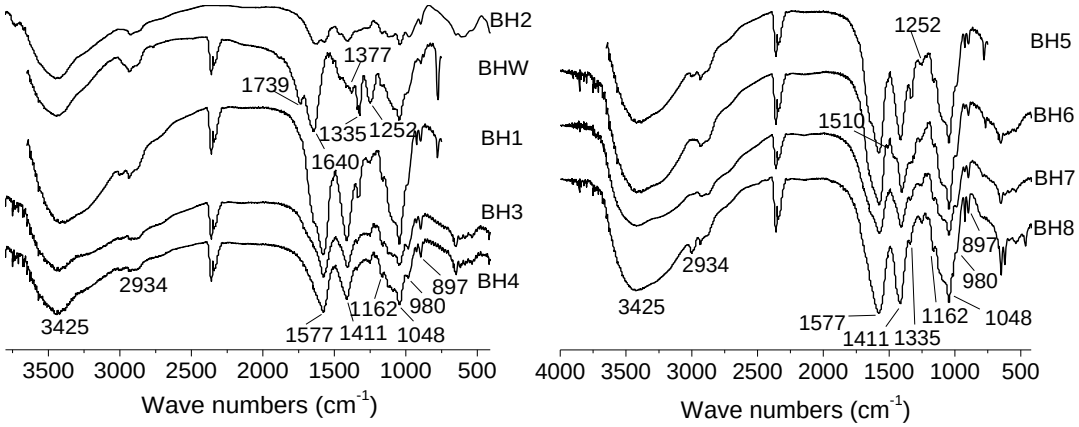

Fig. 2. FT-IR spectra of water-soluble hemicellulosic fraction BHW and alkali-soluble hemicellulosic fractions BH1, BH2, BH3, BH4, BH5, BH6, BH7, and BH8

The prominent absorption around 1048 cm^{-1} was attributed to the C–O, C–C stretching or C–OH bending in arabinoxylans (Kačuráková et al.1994). The low intensity of the band at 980 cm^{-1} indicated the presence of arabinose attached at the position O-3 of the xylopyransyl constituents (Ebringerová et al. 1992). As shown in Fig. 2, the typical signal characteristics of the spectra of nine hemicellulosic fractions were similar, except for the different intensity of the absorption at typical signals. FTIR analysis indicated that the hemicelluloses from bamboo culm were likely to contain arabinoxylans and a small quantity of lignin.

Thermal Analysis

The TG-DTG curves for the hemicellulosic fractions at a heating rate of 10 °C/min are shown in Fig. 3, and the results are given in Tables 3 and 4. As can be seen from Fig. 3, the pyrolysis process with the increase of temperature could be simply divided into three stages. The first stage was ascribed to the loss of moisture and volatile ingredients, the second stage was attributed to fast thermal decomposition, and the third stage represented the degradation of volatile components and further charring processes of the residues with lignin decomposition occurring over a wide temperature range (Sun et al. 2011). In the second stage, a significant loss of sample mass occurred, varying from 23.07% to 50.99% of the original weight (Table 3). The mass losses of fractions being separated out in solution at pH lower than 5.5 (BH1, BH2, BH3, and BH4) were higher than those of fractions remaining soluble in alkaline solution at pH even lower than 5.5 (BH5, BH6, BH7, and BH8). The fraction BH1 had the highest mass loss of 50.99%, and the fraction BH8 had the lowest one. As illustrated, the nine hemicellulose fractions began to decompose at significant rates when the temperature was higher than 187 °C. The variations in initial degradation temperatures were related to the differences in the elemental and chemical compositions of the samples (Mansaray and Ghaly 1999). The peak temperatures at maximum rate of weight loss occurred at 253, 284, 275, 267, 276, 263, 260, 263, and 275 °C for BHW, BH1, BH2, BH3, BH4, BH5, BH6, BH7, and BH8, respectively (Fig. 3). The peak temperatures were within a narrow range of 253 to 284 °C. The corresponding maximum mass loss rates were 7.94, 7.27, 4.61, 6.68, 8.64, 3.85, 5.15, 5.78, and 7.06%/min (Table 4). The differences of peak temperature and maximum rate of weight loss in the main degradation stage were possibly owing to the structural inhomogeneity of the fractions and mutual differences in the relative content of the constituents (Sun et al. 2011). The shoulder peaks in DTG curves were observed at 220, 217, 204, 205, and 217 °C, respectively, for BH1, BH2, BH3, BH7, and BH8 in the major degradation zone (Fig. 3). According to Yang et al. (2007), cellulose and hemicellulose decompose between 200 and 400 °C, releasing CO_2 and CO respectively. Also according to Liu et al. (2011), the influences of lignin on hemicellulose are significant during pyrolysis, and hemicellulose contributes the most to the mass loss rate at temperature below 327 °C, while lignin contributes the least to the mass loss before 327 °C. Referring to the study by Rousset et al. (2009), the structure, content, and mode of assembly of hemicelluloses, lignin, and cellulose have marked effects on the reaction mechanisms during thermal treatment and therefore have a strong influence on the quality of the final product. Thus, in the second stage the weight loss was mainly attributed to the selective loss of the main components of hemicelluloses. Besides, hemicellulosic fractions that are

more highly ramified show a higher thermal stability (Sun et al. 2011). Therefore, in summary, it was likely that the hemicellulosic fraction BH1 maybe had the highest content of hemicelluloses and more ramified polysaccharides, while the fraction BH8 had the highest content of lignin residues. However, based on the DTG curves of BHW, BH3, BH4, BH5, BH7, and BH8 in the third step, an obvious weight loss was observed between 430 and 537 °C. The temperature peaks with weaker intensity were discovered at 527, 445, 465, 465, 446, and 484 °C respectively, and the corresponding maximum pyrolysis rates were 2.18, 0.91, 1.17, 1.41, 0.87, and 3.25%/min, respectively. The decomposition ranging from 410 to 540 °C was suggested to proceed through the degradation of the volatile components, forming char (Yang et al. 2006, 2007; Sun et al. 2011). In the third step for the samples BH1, BH2, and BH6, further charring process continued with unconspicuous decomposition of the volatile components. The main weight loss step was followed by a low, flat TG signal. Though an obvious weight loss did not appear, the third thermal stage was clearly present, which may be due to a slow step-by-step decomposition (charring) of the residue. The thermal behavior of sample BH3 was similar to that of fraction BH7. Interestingly, in the third stage the peak temperature of water-soluble sample (527 °C) was much higher than those of alkali-soluble hemicelluloses. At the same time, in the third decomposition region the weight of fraction BH8 was discovered to lose most. As a result, at final temperature of 700 °C the total weight losses were 59.21% for BHW, 76.06% for BH1, 75.88% for BH2, 72.89% for BH3, 69.33% for BH4, 59.49% for BH5, 59.65% for BH6, 69.12% for BH7, and 51.89% for BH8, respectively (Table 3). In total, the mass losses of fractions BH5, BH6, BH7, and BH8 were lower than those of fractions BH1, BH2, BH3, and BH4. That is, the thermal stability of hemicellulosic fractions BH5, BH6, BH7, and BH8, appeared to be higher than those of the fractions BH1, BH2, BH3, and BH4, when they were treated under N_2 atmosphere from room temperature to 700 °C at a heating rate of 10 °C. Hemicellulosic fraction BH1 exhibited the lowest thermal stability, while hemicelluloses BH8 was the most difficult to decompose.

Table 3. Temperature Ranges and Weight Losses of Hemicellulosic Fractions

Samples	Stage 1		Stage 2		Stage 3		Total weight loss (%)
	Temperature range (°C)	Weight loss (%)	Temperature range (°C)	Weight loss (%)	Temperature range (°C)	Weight loss (%)	
BHW	< 210	9.06	210-310	30.87	310-700	19.27	59.21
BH1	< 190	8.41	190-320	50.99	320-700	15.66	76.06
BH2	< 200	16.48	200-320	46.70	320-700	12.69	75.88
BH3	< 191	15.15	191-310	41.94	310-700	15.80	72.89
BH4	< 200	15.03	200-315	38.92	315-700	15.37	69.33
BH5	< 193	12.28	193-330	29.67	330-700	17.53	59.49
BH6	< 193	9.61	193-346	35.44	346-700	14.60	59.65
BH7	< 187	14.24	187-316	38.60	316-700	16.28	69.12
BH8	< 193	6.14	193-327	23.07	327-700	22.67	51.89

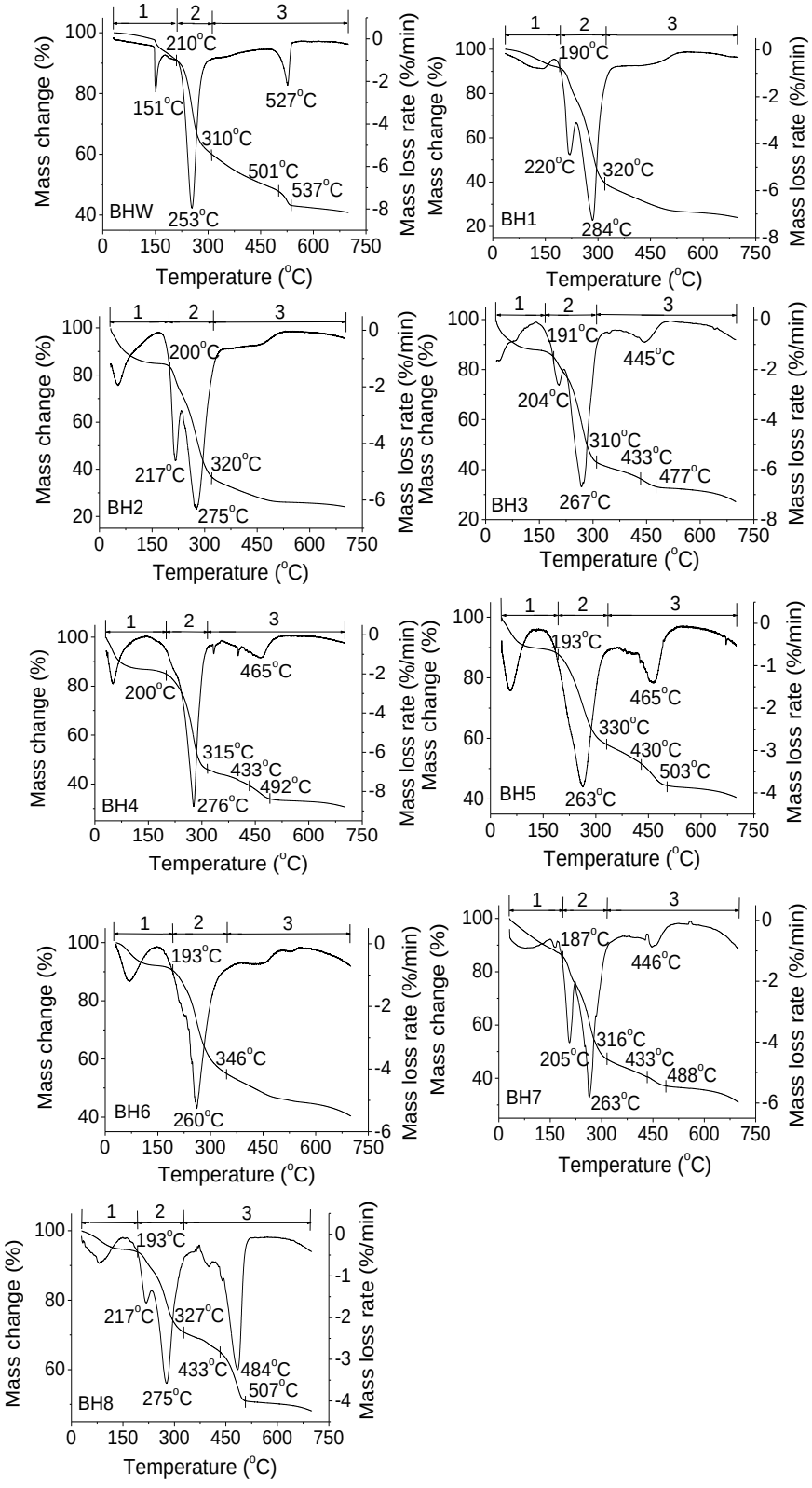

Fig. 3. TG-DTG curves of the hemicellulosic fractions at the heating rate of 10 °C/min

Table 4. Peak Temperatures and Maximum Weight Loss Rates of the Hemicellulosic Fractions during Stage 2 and Stage 3

Samples	Stage 2		Stage 3	
	T_{peak} (°C)	Maximum weight loss rate (%/min)	T_{peak} (°C)	Maximum weight loss rate (%/min)
BHW	253	7.94	527	2.18
BH1	284	7.27	-	-
BH2	275	4.61	-	-
BH3	267	6.68	445	0.91
BH4	276	8.64	465	1.17
BH5	263	3.85	465	1.41
BH6	260	5.15	-	-
BH7	263	5.78	446	0.87
BH8	275	3.56	484	3.25

It has been reported that the higher proportion of non-sugar components (mainly lignin) in the fraction and the higher molecular weight of hemicelluloses resulted in a higher thermal stability (Li et al. 2011; Chen et al. 2010; Jin et al. 2009). Besides, lignin contributes the most to the residues above 327 °C (Liu et al. 2011). Linking the cited works (Rousset et al. 2009; Sun et al. 2011; Li et al. 2011; Chen et al. 2010; Jin et al. 2009; Liu et al. 2011) with the present results, it was concluded that their thermal diversity was possibly caused mainly by their different presence of associated lignin content in hemicellulosic fraction, as well as different chemical structure and molecular weight of hemicelluloses.

Kinetic Analysis of Hemicellulose Pyrolysis

Thermal kinetics in the first stage, which was due to the loss of moisture and highly volatile matter, was not considered in detail here. Moreover, compared with those in the second stage, the weight losses occurred over a wide temperature range corresponding to the decomposition of lignin and other volatile components the third stage. Thus, only the thermal kinetic model of the main decomposition process will be discussed, dealing with the pyrolysis characteristics.

Lignocellulosic biomass is mainly composed of macromolecular compounds, so each step of pyrolysis can be considered to be a single reaction according to Coats-Redferm method (Coats and Redfern 1964). According to the TG curve, the conversion ratio of hemicelluloses a is defined in Eq.1,

$$a = \frac{m_0 - m_T}{m_0 - m_\infty} \quad (1)$$

where m_0 is the initial sample mass, m_T is the instantaneous mass at temperature T, and m_∞ is the residue mass at the end of process.

Hence the decomposition rate equation can be described as follows,

$$\frac{da}{dt} = Kf(a) \quad (2)$$

where K is the reaction rate constant and $f(a)$ is the differential form of kinetic mechanism function. According to the Arrhenius correlation, the rate constant is derived,

$$K = A e^{-E/RT} \quad (3)$$

where A (min^{-1}) is pre-exponential factor, E (J/mol) is activation energy, R is the gas constant (R=8.314 J/mol·K), and T is thermodynamic temperature. Thus we can write Eq. 4 as,

$$f(a) = (1-a)^n \quad (4)$$

where n is the reaction order. The pyrolytic behaviour of lignocellulosic biomass including hemicelluloses can be assumed to follow first order reactions (Varhegyi et al. 1989). Thus, after inserting Eq. 3 and Eq. 4 into Eq. 2, Eq. 5 is obtained in the following form:

$$\frac{da}{dt} = A e^{-E/RT} (1-a) \quad (5)$$

When the TG heating rate $r=dT/dt$ is incorporated in Eq. 5, Eq. 6 can be written as

$$\frac{da}{dT} = \frac{A}{r} e^{-E/RT} (1-a) \quad (6)$$

Integration of Eq. 6 yields:

$$\ln\left(\frac{-\ln(1-a)}{T^2}\right) = \ln\left(\frac{AR}{rE}\left(1 - \frac{2RT}{E}\right)\right) - \frac{E}{RT} \quad (7)$$

As the term of $2RT/E \approx 0$ can be neglected, since it is much less than 1 for the single reaction process in this analytical method, Eq. 7 can be simplified as Eq. 8:

$$\ln\left(\frac{-\ln(1-a)}{T^2}\right) = \ln\left(\frac{AR}{rE}\right) - \frac{E}{RT} \quad (8)$$

The terms of $\ln(-\ln(1-a)/T^2)$ vary linearly with $1/T$, and the slope of the line is minus E/R. At the same time, the intercept of the line with y-axis is $\ln(AR/rE)$. Both the activation energy E and pre-exponential factor A can be determined by the slope and intercept of the lines. The obtained linearization curves of the hemicelluloses are given in Fig. 4. The corresponding parameters within main pyrolysis temperature ranges were obtained as listed in Table 5. However, each step of pyrolysis was considered to be a single reaction, thus, the calculated value of activation energy was an average value.

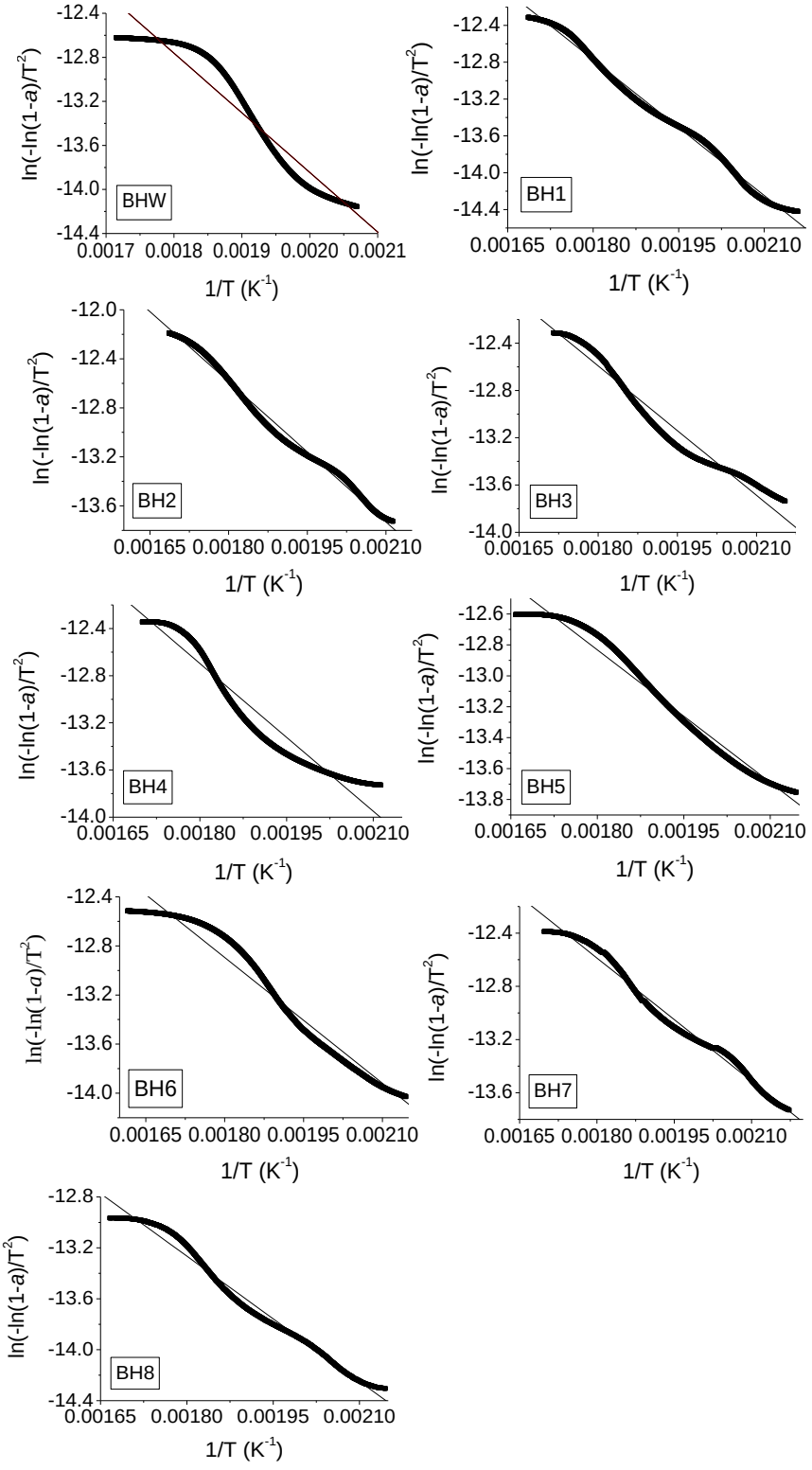

Fig. 4. Linearization curves of the hemicellulosic fractions at the heating rate of 10 °C/min

As shown in Fig. 4, the relationships between $1/T$ and $\ln(-\ln(1-a)/T^2)$ for BH1, BH2, BH3, BH5, BH7, and BH8 were obviously linear. The model of a single reaction gave a good fit to the experimental data with good R^2 value (Table 5). But in the case of the single reaction model, the fits were worse for BHW, BH4, and BH6 to some degree. Some studies have described the thermal decomposition of xylan and related model compounds by a chain of two successive reactions (Varhegyi et al. 1989; Di Blasi and Lanzetta 1997; Ramiah 1970). Obviously we could not exclude the existence of two or more successive reactions for the bamboo hemicelluloses BHW, BH4, and BH6. Our experiments, however, could also reflect the thermal kinetic parameters of complex hemicelluloses.

Within the main pyrolysis temperature range, the activation energy of BHW, BH1, BH2, BH3, BH4, BH5, BH6, BH7, and BH8 were 45.02, 40.85, 31.69, 30.34, 34.73, 23.77, 28.37, 25.66, and 27.27 kJ/mol, respectively (Table 5). The activation energy was within the range of 23 to 45 kJ/mol. It was observed that the activation energy values were similar with those of most agricultural residues or native lignin investigated in previous studies (Wen et al. 2011; Slovak and Susak 2004; Liu et al. 2008). The activation energy values of fractions BH1, BH2, BH3, and BH4, which were soluble in solution only at pH higher than 5.5, were higher than those of fractions kept at pH lower than 5.5 and being precipitated in three volumes of 95% ethanol (BH5, BH6, BH7, and BH8). The tendency of the pre-exponential factors *A* almost coincided with the principle of activation energy. Highest activation energy and pre-exponential factor were found for the water-soluble fraction (45.02 kJ/mol and 2655.81 min^{-1}, respectively). The kinetic parameters including activation energy and pre-exponential factor were much lower than the values in the literature as given in Table 6. Referring to the results obtained by Yang et al. (2004), the energy for lignin is only ca. 30 kJ/mol based on a first order reaction mechanism. The kinetic parameters seemed probably to show a kinetic compensation effect because of the existence of lignin. It is well documented in the literature that biomass reactivity is based on physical, structural, and elemental characteristics of individual components (Mckendry 2002; Rhen et al. 2007; Yang et al. 2004). Thus, the different chemical structure and molecular weight of hemicelluloses and the different content of associated lignin may possibly be responsible for the different thermal kinetics parameters of pyrolysis among the bamboo hemicelluloses.

Table 5. Kinetics Parameters of Pyrolysis of the Hemicellulosic Fractions

Sample	Temperature (°C)	Linear regression equation	*E* (kJ/mol)	*A* (min^{-1})	R^2
BHW	210-310	Y=-5414.82467X-3.01529	45.02	2655.81	0.930
BH1	190-320	Y=-4913.87974X-3.92830	40.85	967.30	0.994
BH2	200-320	Y=-3812.14643X-5.72541	31.69	124.43	0.991
BH3	191-310	Y=-3649.39354X-6.02338	30.34	88.42	0.968
BH4	200-315	Y=-4177.72528X-5.17636	34.73	236.11	0.945
BH5	193-330	Y=-2859.58507X-7.68454	23.77	13.16	0.974
BH6	193-346	Y=-3412.11484X-6.75295	28.37	39.86	0.959
BH7	187-316	Y=-3085.99955X-7.03223	25.66	27.27	0.987
BH8	193-327	Y=-3280.26618X-7.36053	27.27	20.87	0.985

R^2 is the coefficient of determination. R^2 of 1 indicates a perfect fit.

Table 6. First Order Reaction Parameters of Hemicellulose Pyrolysis in Previous Studies

Sample	Heating rates	Temperature (°C)	E (kJ/mol)	A (min^{-1})	Literature
200 mg potassium xylan (30-50 μm)	Isothermal	215-250	125.58	1.32×10^{11}	Ramiah 1970
2-4 mg of commercial xylan	20 K/min	473-673	72.00	1.2×10^{6}	Bilbao et al. 1989
Xylan	10 °C/min	220-300	69.36	1.26×10^{5}	Yang et al. 2004

CONCLUSIONS

1. In the present study, water-soluble hemicelluloses (BHW) and eight alkali-soluble hemicellulosic fractions BH1 to BH8 were obtained from bamboo (*Phyllostachys-pubescens Mazel*) culm, totally yielding 67.61%. Extraction with NaOH solution resulted in higher hemicellulose yield.
2. All the hemicelluloses possibly contained arabinoxylans associated with small amounts of lignin, according to FTIR analysis.
3. The weight loss of hemicelluloses during pyrolysis process mainly occurred within the interval 187 to 346 °C. The maximum mass loss rate ranged from 3.56 to 8.64%/min in the major weight loss temperature range with peak temperature ranging from 253 to 284 °C. The fractions being soluble in solution only at pH higher than 5.5 (BH1, BH2, BH3, and BH4) had a relatively lower thermal stability compared to the fractions being precipitated in ethanol (BH5, BH6, BH7, and BH8). The 2% NaOH-soluble fraction BH1 was found to have the lowest thermal stability, while fraction BH8 exhibited a contrary behavior.
4. Based on first-order reaction kinetics, the activation energy and the pre-exponential factors of the hemicelluloses in the major pyrolysis stage ranged from 23.77 to 45.02 kJ/mol and 13.16 to 2655.81 min^{-1}, respectively. The hemicelluloses BH1, BH2, BH3, and BH4 exhibited higher values of activation energy and pre-exponential factor than hemicelluloses BH5, BH6, BH7, and BH8. The inherent variations in the chemical structure of different samples were likely to play an important role in their thermal difference.
5. The developed thermal characteristics could provide a good evaluation on the thermal degradation of bamboo hemicelluloses. The knowledge thus could be useful for designing thermal processes of bamboo in industry.

ACKNOWLEDGMENTS

The authors are grateful for financial support of the Natural Science Foundation of China (30960304), Natural Science Foundation from Ministry of Education of Jiangxi Province of China (GJJ10045).

REFERENCES CITED

Bilbao R., Millera R. A., and Arauzo J. (1989). "Kinetics of weight loss by thermal decomposition of xylan and lignin, influence of experimental conditions," *Thermochim. Acta.* 143, 137-148.

Chaa, L., Joly, N., Lequart, V., Faugeron, C., Mollet, J. C., Martin, P., and Morvan, H. (2008). "Isolation, characterization and valorization of hemicelluloses from *Aristidapungens* leaves as biomaterial," *Carbohyd. Polym.*74(3), 97-602.

Chen, W. H., Tu, Y. J., and Sheen, H. K. (2010). "Impact of dilute acid pretreatment on the structure of bagasse for bioethanol production," *Int. J. Energ Res*. 34(3), 265-274.

Coats, A. W., and Redfern, J. P. (1964). "Kinetic parameters from thermogravimetric data," *Nature* 201(4914), 68-69.

Di Blasi, C., Lanzetta M. (1997). "Intrinsic kinetics of isothermal xylan degradation in inert atmosphere," *J. Anal. Appl. Pyrolysis* 40-41, 287-303.

Ebringerová, A., Hromádková, Z., Alföldi, J., and Berth, G. (1992). "Structure and solution properties of corn cob heteroxylans," *Carbohyd.Polym.*19(2), 99-105.

Edashige, Y., and Ishii, T. (1998). "Hemicellulosic polysaccharides from bamboo shoot cell-walls," *Phytochem.* 49(6), 1675-1682.

Gírio, F. M., Fonseca, C., Carvalheiro, F., Duarte, L. C., Marques S., and Bogel-Lukasik R. (2010). "Hemicelluloses for fuel ethanol: A review," *Bioresourc. Technol.* 101(13), 4775-4800.

Huang, H. J., Ramaswamy, S., Tschirner, U. W., and Ramarao, B. V. (2008). "A review of separation technologies in current and future biorefineries," *Sep. Purif. Technol.* 62(1), 1-21.

Jin, A. X., Ren, J. L., Peng, F., Xu, F., Zhou, G. Y., Sun R. C., and Kennedy, J. F. (2009). "Comparative characterization of degraded and non-degradative hemicelluloses from barely straw and maize stems: Composition, structure, and thermal properties," *Carbohyd. Polym.* 78(2), 609-619.

Kačuráková, M., Capek, P., Sasinková, V., Wellner, N., and Ebringerová, A. (2000). "FT-IR study of plant cell wall model compounds: Pectic polysaccharides and hemicelluloses," *Carbohyd.Polym.* 43(2), 195-203.

Kačuráková, M., Belton, P. S., Wilson, R. H., Hirsch, J., and Ebringerová, A. (1998). "Hydration properties of xylan-type structures: An FT-IR study of xylooligosaccharides," *J. Sci. Food Agric.* 77(1), 38-44.

Kačuráková, M., Ebringerová, A., Hirsch, J., and Hromádková, Z. (1994). "Infrared study of arabinoxylans," *J. Sci. Food Agric.* 66(3), 423-427.

Lawther, J. M., Sun, R. C., and Banks, W. B. (1995). "Extraction, fractionation, and characterization of structural polysaccharides from wheat-straw," *J. Agric. Food. Chem.* 43(3), 667-675.

Li, M. F., Fan, Y. M., Xu, F., and Sun, R. C. (2011). "Structure and thermal stability of polysaccharide fractions extracted from the ultrasonic irradiated and cold alkali pretreated bamboo," *J. Appl. Polym. Sci.* 121(1), 176-185.

Liu, Q., Wang, S. R., Zheng, Y., Luo, Z. Y., Cen, K. F. (2008). "Mechanism study of wood lignin pyrolysis by using TG-FTIR analysis," *J. Anal. Appl. Pyrolysis* 82(1), 170-177.

Liu, Q., Zhong, Z. P., Wang, S. R., and Luo, Z. Y. (2011). "Interaction of biomass components during pyrolysis: ATG-FTIR study," *J. Anal. Appl. Pyrolysis* 90(2), 213-218.

Mansaray, K. G., and Ghaly, A. E. (1999). "Kinetics of the thermal degradation of rice husks in nitrogen atmosphere," *Energ. Sources.* 21(9), 773-784.

Market Report No.11A001. (2001). Market survey on activated carbon industry in China, Guangzhou CCM Chemicals Co.Ltd, China, July.

Mckendry, P. (2002). "Energy production from biomass (Part 1): Overview of biomass," *Bioresourc. Technol.* 83(1), 37-46.

Patwardhan, P. R., Dalluge, D. L., Shanks, B. H., and Brown R. C. (2011). "Distinguishing primary and secondary reactions of cellulose pyrolysis," *Bioresour. Technol.* 102(8), 5265-5269.

Peng, Y. Y., and Wu, S. B. (2010). "The structural and thermal characteristics of wheat straw hemicellulose," *J. Anal. Appl. Pyrolysis.* 88(2), 134-139.

Ramiah, M. V. (1970). "Thermogravimetric and differential thermal analysis of cellulose, hemicellulose, and lignin," *J. Appl. Polym. Sci.* 14(5), 1323-1337.

Revanappa, S. B., Nandini, C. D., and Salimath, P. V. (2010). "Structural characterization of pentosans from hemicellulose B of wheat varieties with varying chapatti-making quality," *Food Chem.* 119(1), 27-33.

Rhén, C., Öhman, M., Gref, R., and Wästerlund, I. (2007). "Effect of raw material composition in woody biomass pellets on combustion characteristics," *Biomass Bioenergy* 31(1), 66-72.

Rousset, P., Aguiar, C., Labbé, N., and Commandré, J. M. (2011). "Enhancing the combustible properties of bamboo by torrefaction," *Bioresourc. Technol.* 102(17), 8225-8231.

Rousset, P., Lapierre, C., Pollet, B., Quirino, W., and Perre, P. (2009). "Effect of severe thermal treatment on spruce and beech wood lignins," *Ann. For. Sci.* 66(1), 110-117.

Scurlock, J. M. O., Dayton, D. C., and Hames, B. (2000). "Bamboo: An overlooked biomass resource?," *Biomass Bioenergy* 19(4), 229-244.

Shanmughavel, P., and Francis, K. (1996). "Above ground biomass production and nutrient distribution in growing bamboo (*Bambusabambos* (L.) Voss)," *Biomass Bioenergy* 10(5-6), 383-391.

Shen, D. K., and Gu S. (2009). "The mechanism for thermal decomposition of cellulose and its main products," *Bioresourc. Technol.* 100(24), 6496-6504.

Shen, D. K., Gu, S., and Bridgwater, A. V. (2010). "Study on the pyrolytic behaviour of xylan-based hemicellulose using TG-FTIR and Py-GC-FTIR," *J. Anal. Appl. Pyrolysis* 87(2), 199-206.

Slovak, V., and Susak, P. (2004). "Pitch pyrolysis kinetics from single TG curve," *J. Anal. Appl. Pyrolysis* 72(2), 249-252.

So, F. Y. S., and Wong, F. K. W. (1998). "Bamboo scaffolding development in Hong Kong – A critical review," In: Proceedings of the Symposium on Bamboo and Metal Scaffolding, Harbour Plaza Hotel, Hong Kong.

Sun, J. X., Sun, X. F., Sun, R. C., and Su, Y. Q. (2004). "Fractional extraction and structural characterization of sugarcane bagasse hemicelluloses," *Carbohyd.Polym.* 56(2), 195-204.

Sun, R. C., Fang, J. M., Tomkinson, J., Geng, Z.C., and Liu, J. C. (2001). "Fractional isolation, physico-chemical characterization and homogeneous esterification of hemicelluloses from fast-growing poplar wood," *Carbohyd.Polym.* 44(1), 29-39.

Sun, R. C., Sun, X. F., and Ma, X. H. (2002). "Effect of ultrasound on the structural and physiochemical properties of organosolv soluble hemicelluloses from wheat straw," *Ultrason. Sonochem.* 9(2), 95-101.

Sun, Y. C., Wen, J. L., Xu, F., and Sun, R. C. (2011). "Structural and thermal characterization of hemicelluloses isolated by organic solvents and alkaline solutions from *Tamarix austromongolica*," *Bioresourc. Technol.* 102(10), 5947-5951.

Varhegyi, G., Antal, M. J., Szekely, T., and Szabo, P. (1989). "Kinetics of the thermal decomposition of cellulose, hemicellulose, and sugarcane bagasse," *Energ. Fuel* 3(3), 329-335.

Vazquez, G., Antorrena, G., Gonzalez, J., and Freire, S. (1997). "FTIR, H-1 and C-13 NMR characterization of acetosolv-solubilized pine and eucalyptus lignins," *Holzforschung* 51(2), 158-166.

Velmurugan, R., and Muthukumar, K. (2011). "Utilization of sugarcane bagasse for bioethanol production: Sono-assisted acid hydrolysis approach," *Bioresourc. Technol.* 102(14), 7119-7123.

Wen, J. L., Xiao, L. P., Sun, Y. C., Sun, S. N., Xu, F., Sun, R. C., and Zhang, X. L. (2011). "Comparative study of alkali-soluble hemicelluloses isolated from bamboo (*Bambusarigida*)," *Carbohyd. Res.* 346(1), 111-120.

Xiao, B., Sun, X. F., and Sun, R. C. (2001). "Chemical, structural, and thermal characterizations of alkali-soluble lignins and hemicelluloses, and cellulose from maize stems, rye straw, and rice straw," *Polym.Degrad. Stabil.*74(2), 307-319.

Xu, Y. X., and Hanna, M. A. (2010). "Optimum conditions for dilute acid hydrolysis of hemicellulose in dried distillers grains with solubles," *Ind. Crop. Prod.* 32(3), 511-517.

Yang, H. P., Yan, R., Chen, H. P., Hee, D. H., and Zheng, C. G. (2007). "Characteristics of hemicellulose, cellulose and lignin pyrolysis," *Fuel* 86(12-13), 1781-1788.

Yang, H. P., Yan, R., Chen, H. P., Zheng, C. G., Lee, D. H., and Liang, D. T. (2006). "In-depth investigation of biomass pyrolysis based on three major components: Hemicellulose, cellulose and lignin," *Energ. Fuel* 20(1), 388-393.

Yang, H. P., Yan, R., Chin, T., Liang D. T., Chen, H. P., and Zheng, C. G. (2004). "Thermogravimetric analysis-Fourier transform infrared analysis of palm oil waste pyrolysis," *Energ. Fuel* 18(6), 1814-1821.

Yu, Z. S., Ma, X. Q., and Liu A. (2008). "Kinetic studies on catalytic combustion of rice and wheat straw under air- and oxygen-enriched atmospheres, by using thermogravimetric analysis," *Biomass Bioenergy* 32(11), 1046-1055.

Article submitted: September 22, 2011; Peer review completed: October 23, 2011; Revised version received and accepted: November 15, 2011; Published: November 17, 2011.